IEEE Trans. on Microwave Theory and Techniques, 40(7):1496–1506, July 1992.

Fast Capacitance Extraction of General Three-Dimensional Structures

K. Nabors S. Kim J. White

Abstract

In [1], a boundary-element based algorithm was presented for computing the capacitance of three-dimensional m-conductor structures whose computational complexity grows nearly as mn, where n is the number of elements used to discretize the conductor surfaces. In that algorithm, a generalized conjugate residual iterative technique is used to solve the $n \times n$ linear system arising from the discretization, and a multipole algorithm is used to compute the iterates. In this paper, several improvements to that algorithm are described which make the approach in [1] applicable and computationally efficient for almost any geometry of conductors in a homogeneous dielectric. In particular, a new adaptive multipole algorithm is described, along with a strategy for accelerating the iterative algorithm by exploiting electrostatic screening. Results using these techniques in a program which computes the capacitance of general three-dimensional structures are presented to demonstrate that the new algorithm is nearly as accurate as the more standard direct factorization approach, and is more than two orders of magnitude faster for large examples.

I. Introduction

In the design of high performance integrated circuits and integrated circuit packaging, there are many cases where accurate estimates of the capacitances of complicated three-dimensional structures are important for determining final circuit speeds and functionality. Algorithms using method of moments [2] or weighted-residuals [3, 4] based discretizations of integral equation formulations, also known as boundary-element methods [5], are commonly used to compute these capacitances, but such approaches generate dense matrix problems

Manuscript received April 12, 2011. This work was supported by the Defense Advanced Research Projects Agency contracts N00014-91-J-1698 and MDA972-88-K-008, the National Science Foundation contract (MIP-8858764 A02), F.B.I. contract J-FBI-88-067, and grants from Digital Equipment Corporation and I.B.M.

The authors are with the Research Laboratory of Electronics and the Microsystems Technology Laboratory, Department of Electrical Engineering and Computer Science, Massachusetts Institute of Technology, Cambridge, MA 02139 U.S.A., (617) 253-2543.

which are computationally expensive to solve, and this limits the complexity of problems which can be analyzed.

In [1], a fast algorithm for computing the capacitance of three-dimensional structures of rectangular conductors in a homogenous dielectric is presented. The method solves the discretized capacitance problem using an iterative technique with iterates computed by a hierarchical multipole algorithm [6, 7]. This general strategy was first suggested in [8]. The computation time for the algorithm was shown to grow nearly as mn, where n is the number of panels used to discretize the conductor surfaces, and m is the number of conductors. In this paper, we describe several improvements to that algorithm and present computational results on a variety of examples to demonstrate that the new method is accurate and can be as much as two orders of magnitude faster than standard direct factorization approaches.

The outline of the paper is as follows. The boundary-element formulation and a standard iterative algorithm for solving the generated matrix problem are briefly reviewed in Section II. A simplified version of the hierarchical multipole algorithm is described in Section III, and our new adaptive multipole algorithm tuned to the boundary-element formulation is given in Section IV. A new preconditioning strategy for accelerating the iterative algorithm, based on the idea of screening, is presented in Section V. Experimental results using our program FASTCAP to analyze a wide variety of structures, made possible by a link to the M.I.T. Micro-Electro-Mechanical Computer Aided Design (MEMCAD) system [9], are presented in Section VI. Finally, conclusions and acknowledgements are given in Section VII.

II. Problem Formulation

Capacitance extraction is made tractable by assuming the problem contains conductors embedded in a homogenous dielectric medium, though the techniques described below can be extended to the piecewise-constant dielectric case using the approach in [10]. The capacitance of an m-conductor geometry can then be summarized by an $m \times m$ symmetric matrix C, where the j-th column of C has a positive entry C_{jj}, representing the self-capacitance of conductor j, and negative entries C_{ij}, representing coupling between conductors j and i, $i = 1, 2, \ldots, m$, $i \neq j$. To determine the j-th column of the capacitance matrix, one need only solve for the surface charges on each conductor produced by raising conductor j to one volt while grounding the rest. Then C_{ij} is numerically equal to the charge on conductor i, $i = 1, 2, \ldots, m$. Repeating this procedure m times gives the m columns of C.

These m potential problems can be solved using an equivalent free-space formulation in which the conductor-dielectric interfaces are replaced by a charge layer of density σ [11, 10]. Assuming a homogenous dielectric, the charge layer in the free-space problem will be the induced charge in the original problem if σ satisfies the integral equation

$$\psi(x) = \int_{surfaces} \sigma(x') \frac{1}{4\pi\epsilon_0 \|x - x'\|} da', \qquad x \in surfaces. \tag{1}$$

where $\psi(x)$ is the known conductor surface potential, da' is the incremental conductor surface area, x, $x' \in \mathbf{R}^3$, and $\|x\|$ is the usual Euclidean length of x given by $\sqrt{x_1^2 + x_2^2 + x_3^2}$.

A standard approach to numerically solving (1) for σ is to use a piece-wise constant collocation scheme. That is, the conductor surfaces are broken into n small panels or tiles,

and it is assumed that on each panel i, a charge, q_i, is uniformly distributed. Then for each panel, an equation is written which relates the known potential at the center of that i-th panel, denoted $\overline{p}_i$, to the sum of the contributions to that potential from the n charge distributions on all n panels [10]. The result is a dense linear system,

$$Pq = \overline{p} \tag{2}$$

where $P \in \mathbf{R}^{n\times n}$, q is the vector of panel charges, $\overline{p} \in \mathbf{R}^n$ is the vector of known panel potentials, and

$$P_{ij} = \frac{1}{a_j} \int_{panel_j} \frac{1}{4\pi\epsilon_0 \|x_i - x'\|}\, da', \tag{3}$$

where x_i is the center of the i-th panel and a_j is the area of the j-th panel. Since the discretiztion uses point collocation, in general $P_{ij} \neq P_{ji}$, that is P is unsymmetric.

The dense linear system of (2) can be solved to compute panel charges from a given set of panel potentials, and the capacitances can be derived by summing the panel charges. If Gaussian elimination is used to solve (2), the number of operations is order n^3. Clearly, this approach becomes computationally intractable if the number of panels exceeds several hundred. Instead, consider solving the linear system (2) using a conjugate-residual style iterative method like GMRES [12]. Such methods have the form given below:

Algorithm 1: GMRES algorithm for solving (2)
Make an initial guess to the solution, q^0.
Set $k = 0$.
do {
  Compute the residual, $r^k = \overline{p} - Pq^k$.
  if $\|r\| < tol$, return q^k as the solution.
  else {
    Choose α's and β in
      $q^{k+1} = \sum_{j=0}^{k} \alpha_j q^j + \beta r^k$
    to minimize $\|r^{k+1}\|$.
    Set $k = k + 1$.
  }
}

The dominant costs of Algorithm 1 are in calculating the n^2 entries of P using (3) before the iterations begin, and performing n^2 operations to compute Pq^k on each iteration. Described below is our adaptive hierarchical multipole algorithm which, through the use of carefully applied approximations, avoids forming most of P and reduces the cost of forming Pq^k to order n operations. This does not necessarily imply that each iteration of the GMRES algorithm can be computed with order n operations. If the number of GMRES iterations required to achieve convergence approaches n, then to perform the minimization in each GMRES iteration will require order n^2 operations. This problem is avoided through the use of a preconditioner, also described below, which reduces the number of GMRES iterations required to achieve convergence to well below n for large problems.

III. The Hierarchical Multipole Algorithm

A complete description of the hierarchical multipole algorithm is not given here; the original description is in [6, 7], and its application to capacitance extraction is described in [1]. Instead we describe the expansion approximation and examine a simplified two-dimensional example which both exhibits the method's salient features, and motivates the adaptive algorithm and the preconditioner described in subsequent sections.

3.1. Multipole Expansions

Multipole expansions are often used to approximate the far field due to a confined charge distribution [13]. For example, consider evaluating the potential p_i at the center of a panel i, (r_i, ϕ_i, θ_i), due to a collection of d distant panels, as in Figure 1. The potential due to the surface charges on those d panels is given approximately by the truncated multipole expansion

$$\psi(r_i, \phi_i, \theta_i) \approx \sum_{n=0}^{l} \sum_{m=-n}^{n} \frac{M_n^m}{r_i^{n+1}} Y_n^m(\phi_i, \theta_i) \tag{4}$$

where the spherical coordinates of the evaluation location are measured relative to the origin of the multipole expansion, $Y_n^m(\phi_i, \theta_i)$ are the surface spherical harmonics, M_n^m are the multipole coefficents determined from the panel charges, and l is the expansion order.

Given the multipole coefficients, the same multipole expansion can be used to quickly, but approximately, evaluate the potential at many panel centers. For example, in Figure 1, there are d charged panels, and d panel centers where the potential must be evaluated. A direct calculation of those potentials requires order d^2 operations, but only order d operations are needed if the multipole expansion is used (assuming the expansion order l is fixed).

In the Figure 1 case, the error due to truncating the multipole expansion is bounded [7], as in

$$\left| \psi(r_i, \phi_i, \theta_i) - \sum_{n=0}^{l} \sum_{m=-n}^{n} \frac{M_n^m}{r_i^{n+1}} Y_n^m(\phi_i, \theta_i) \right| \leq K_1 \left(\frac{R}{r_i} \right)^{l+1} \leq K_1 \left(\frac{R}{r} \right)^{l+1}. \tag{5}$$

The quantities r and R are as in Figure 1 and K_1 is a constant independent of the multipole expansion order, l. The bound indicates that the multipole potential evaluations converge more rapidly with expansion order as the minimum distance between the panel charges and the evaluation points increases.

In order to ensure that the error bound in (5) tightens sufficiently with each increase in expansion order l, the hierarchical multipole algorithm uses a multipole expansion to represent the effect of charge in a region only if the radius of the region, R, is less than half the distance between the region's center and the evaluation point, denoted r. For example, in Figure 2 two groups of panels are represented by a multipole expansions of order l, and by the above criteria, both can be used to evaluate the potential at panel i's center, as $R/r = 3R/3r < 0.5$.

3.2. A Two-Dimensional Example

The aggregation of distant tiles into multipole expansions which can be used to evaluate potentials at many panel centers is the source of the hierarchical multipole algorithm's efficiency. Maintaining this efficiency for general distributions of panels while controlling error

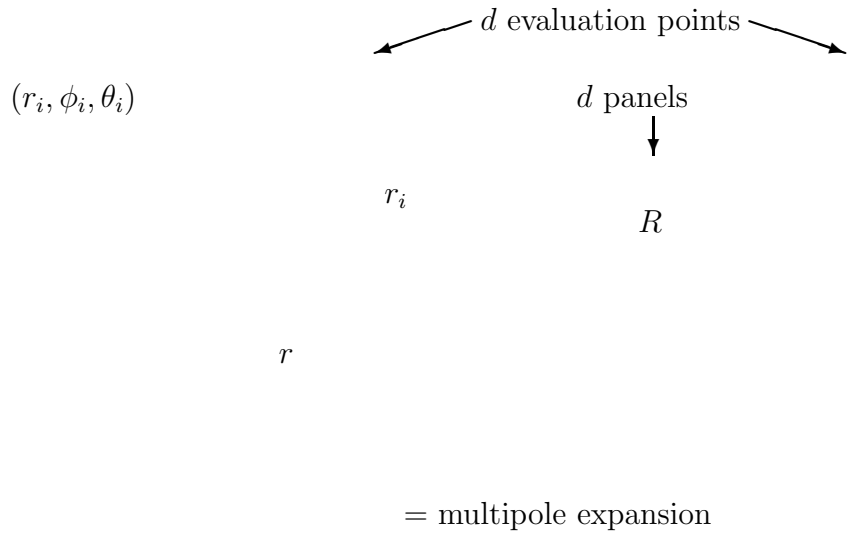

Fig. 1. The evaluation of the potential at (r_i, ϕ_i, θ_i).

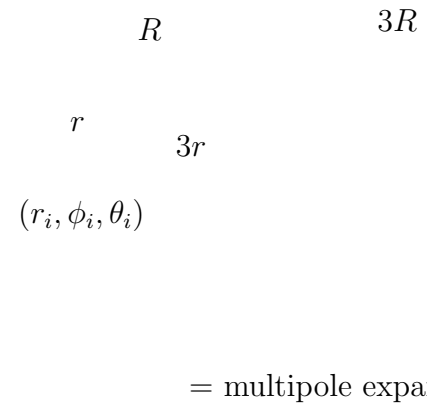

Fig. 2. The evaluation of two multipole expansions with the same error bound.

is ensured by exploiting a hierarchical partitioning of the problem domain, the smallest cube containing all the conductors.

Consider, for example, evaluating the potential at some point (r_i, ϕ_i, θ_i) in Figure 3 due to panel charges inside the illustrated problem domain. A first partitioning would be to break the problem into four smaller squares, leaving (r_i, ϕ_i, θ_i) somewhere in the lower left square (Figure 3b)[1]. To ensure that the errors due to truncating the multipole expansion shrink rapidly with increasing expansion order, multipole expansions will not be used to represent the charges in squares 1, 2 and 3, when evaluating the potential at points in the lower-left square, because R_1/r_1, R_2/r_2 and R_3/r_3 in Figure 3b are all greater than 0.5. For the particular example evaluation point in the lower-left square, the charge in square 2 is distant enough to satisfy the criteria for using multipole expansions. However, a more detailed study of the hierarchical multipole algorithm than we will consider here would show that it is not efficient to exploit such special cases.

Squares 1, 2 and 3 are each divided into four squares, as in Figure 3c, to produce smaller regions which can possibly satisfy the criteria for representation by a multipole expansion. In fact, many of the smaller squares do satisfy the criteria, as can be seen by examining the illustrated case, for which R/r is less than 0.5. Thus, at the end of this partitioning step, all the charges in the squares marked with an M in Figure 3c will be represented with a multipole expansion when evaluating the potential at points in the square containing (r_i, ϕ_i, θ_i).

In order for the multipole expansions to be used to represent the potential due to panel charges contained in the unmarked squares of Figure 3c, these squares are partitioned further, as in Figure 3d. Then, as before, the distance criteria implies that multipole expansions can be used to represent the panel charges in all but a few squares near the square containing the evaluation point. If it is determined not to partition any further than is indicated in Figure 3d, the potential p_i, at (r_i, ϕ_i, θ_i), can then be computed by summing a "near" or direct term and a "far" or multipole term. That is, the "near" contribution to p_i is due to panel charges in the nine unmarked squares in Figure 3d, and is computed directly from $P_{ij}q_j$ products. The "far" contribution to p_i is due to distant panels charges and is determined by evaluating the 25 mulitpole expansions indicated in Figure 3d. In the next section, we will refer to the list of squares associated with those 25 multipole expansions as the *multipole list* for the square containing (r_i, ϕ_i, θ_i).

In general, the number of partitioning levels, L, for a given problem domain is selected so that the squares on the finest level each have no more than k panels (typically k is of the order of ten). Then for a uniform distribution of panels, the number of partitioning levels will be given by $L = \log \frac{n}{k}$. Since the number of multipole expansions on each partitioning level which contribute to p_i is bounded by a constant, each potential evaluation involves order $\log n$ multipole expansion evaluations. Also, since each lowest level square has no more than k panels, the direct contribution to p_i is bounded by a constant. Therefore, as evaluating the entire potential vector requires n evaluations of this type, the above multipole approach is an order $n \log n$ algorithm for computing an approximation to Pq.[2] The hierarchical multipole algorithm given in [7], and used in the FASTCAP program described below, is

[1] In the three-dimensional problem, the equivalent partitioning would be to divide a cube into eight smaller cubes.

[2] The analysis is similar for the three-dimensional case. The primary difference is that in the three-

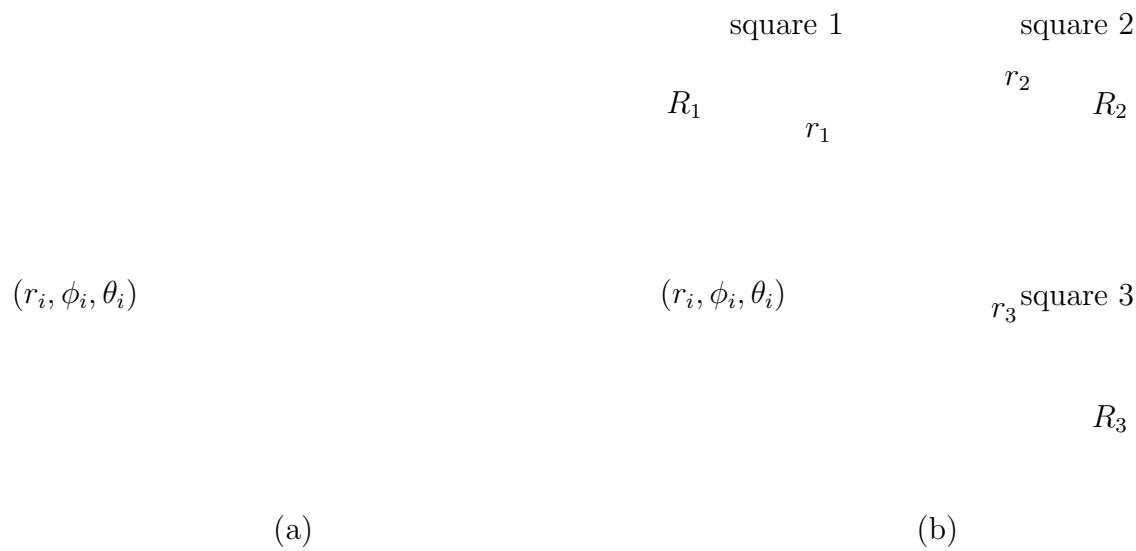

Fig. 3. The evaluation of the potential at (r_i, ϕ_i, θ_i).

more sophisticated than the above approach suggests. In particular, multipole evaluations are efficiently combined into local expansions in such a way as to reduce the number of operations to order n. However, for purposes of describing the adaptive algorithm and the preconditioning techniques below, the simplified algorithm above is sufficiently detailed.

IV. Boundary-Element Oriented Adaptive Calculation

In general, when representing the charge in a region by a multipole expansion, the coefficients M_n^m in (4) are determined from the charge density, $q(\rho, \alpha, \beta)$, as

$$M_n^m = \int_{region} q(\rho, \alpha, \beta) \rho^n Y_n^{-m}(\alpha, \beta) da'. \tag{6}$$

In this section, computing the multipole expansion coefficients for panel charges is examined in more detail, and is shown to lead naturally to an adaptive multipole algorithm.

4.1. Computing the Multipole Expansions

Returning to Figure (1), the potential at the Cartesian equivalent of (r_i, ϕ_i, θ_i), (x_i, y_i, z_i), due to d distant panels may be approximated with a zeroth-order multipole expansion, which is equivalent to computing the potential due to a single charge equal to the sum of the d panel charges, and located at the center of the smallest ball enclosing the panels,

$$\psi(x_i, y_i, z_i) \approx \bar{M}_0^0 \frac{1}{r_i}. \tag{7}$$

Here (x_i, y_i, z_i) is the i-th panel's center point relative to the center of the smallest ball enclosing the distant panels, $r_i \triangleq \sqrt{x_i^2 + y_i^2 + z_i^2}$, and

$$\bar{M}_0^0 \triangleq \sum_{j=1}^{d} q_j. \tag{8}$$

The approximation

$$\psi_0(x_i, y_i, z_i) \triangleq \bar{M}_0^0 \frac{1}{r_i} \tag{9}$$

is the zeroth-order multipole expansion for the potential due to the distant panels. For accuracy reasons, higher order expansions are typically used. For example, the first-order multipole expansion for ψ is

$$\psi(x_i, y_i, z_i) \approx \psi_0(x_i, y_i, z_i) + \psi_1(x_i, y_i, z_i), \tag{10}$$

with

$$\psi_1(x_i, y_i, z_i) \triangleq \bar{M}_1^0 \frac{z_i}{r_i^3} - \bar{M}_1^1 \frac{x_i}{2r_i^3} - \tilde{M}_1^1 \frac{y_i}{2r_i^3}, \tag{11}$$

dimensional case space is partitioned into cubes, and when cubes are subpartitioned, they generate eight smaller cubes.

where, for panels on which the charge is assumed uniformly distributed,

$$\bar{M}_1^0 \triangleq \sum_{j=1}^{d} \frac{q_j}{a_j} \int_{panel_j} z' da'; \tag{12}$$

$$\bar{M}_1^1 \triangleq -2 \sum_{j=1}^{d} \frac{q_j}{a_j} \int_{panel_j} x' da'; \tag{13}$$

$$\tilde{M}_1^1 \triangleq -2 \sum_{j=1}^{d} \frac{q_j}{a_j} \int_{panel_j} y' da'. \tag{14}$$

The added potential ψ_1 is the field due to a single dipole aligned along the vector

$$(x, y, z) = (\bar{M}_1^0, -\bar{M}_1^1/2, -\tilde{M}_1^1/2). \tag{15}$$

In general, the l-th order multipole expansion in (4) can be rewritten in the form

$$\psi(x_i, y_i, z_i) \approx \sum_{n=0}^{l} \psi_n(x_i, y_i, z_i), \tag{16}$$

with each ψ_n cooresponding to the potential due to a 2^n-pole charge constellation.

4.2. The Adaptive Algorithm

The simple multipole algorithm discussed in Section III uses multipole expansions to represent potentials due to panel charges inside cubes which are far enough away from the evaluation point. The efficiency of this procedure depends on the number of panels in the cubes. Consider, for example, a cube containing three panels whose potential is to be approximated using a first-order multipole expansion of the form (16),

$$\psi(x_i, y_i, z_i) \approx \bar{M}_0^0 \frac{1}{r_i} + \bar{M}_1^0 \frac{z_i}{r_i^3} - \bar{M}_1^1 \frac{x_i}{2r_i^3} - \tilde{M}_1^1 \frac{y_i}{2r_i^3}. \tag{17}$$

The exact potential due to the cube's panels has the form

$$\psi(x_i, y_i, z_i) = P_{i1} q_1 + P_{i2} q_2 + P_{i3} q_3, \tag{18}$$

assuming the three panels are numbered 1, 2 and 3. In the capacitance calculation, the geometry-dependent quantities in (17) and (18) are calculated once and stored for repeated use in computing the iterates of Algorithm 1. Thus evaluating (17) involves multiplying four, fixed, geometry-dependent quantities

$$\frac{1}{r_i}, \quad \frac{z_i}{r_i^3}, \quad \frac{x_i}{2r_i^3}, \quad \frac{y_i}{2r_i^3} \tag{19}$$

by the charge-dependent multipole coefficients $\bar{M}_0^0$, $\bar{M}_1^0$, $\bar{M}_1^1$ and $\tilde{M}_1^1$, while (18) involves computing only the three products, multiplying the geometric quantities P_{ij}, $j = 1, \ldots, 3$, by the corresponding charges. Thus evaluating the exact potential from (18) requires one less operation than evaluating the approximate potential using (17), indicating that it will

be more efficient to evaluate the potential due to panels in this cube using $P_{ij}q_j$ products rather by evaluating multipole expansions.

An adaptive multipole algorithm can be derived from the simplified approach described in Section III if the potential due to panel charges in a cube is always evaluated directly, rather than with a multipole approximation, whenever the number of expansion coefficients would exceed the number of panels. A more precise definition of the computational procedure is given in Algorithm 2 below, which uses some notation which we now introduce.

The cube which contains the entire problem domain is referred to as the level 0 cube. If the volume of the cube is divided into eight equally sized child cubes, referred to as level 1 cubes, then each has the level 0 cube as its parent. The panels are distributed among the child cubes by associating a panel with a cube if the panel's center point is contained in the cube. This process can be repeated to produce L levels of cubes, and L partitionings of panels starting with an 8-way partitioning and ending with an 8^L-way partitioning. The number of levels, L, is chosen so that the maximum number of panels in any finest, or L-th, level cube is less than some threshold (nine is a typical default). A neighbor of a given cube is defined as any cube which shares a corner with the given cube or shares a corner with a cube which shares a corner with the given cube (note that a cube has a maximum of 124 neighbors). Finally, in the algorithm below it is assumed that for each finest-level cube, a multipole list has been constructed using a recursive approach similar to that given in the two-dimensional example above.

Algorithm 2: Adaptive Algorithm for Computing $p = Pq$.

```
Comment: Compute the potential due to nearby charges directly.
  For each finest-level cube i = 1 to 8^L {
    For each panel j in finest-level cube i {
      Set p_j = 0.
      For each panel k in cube i or its neighbors {
        Add P_jk q_k to p_j.
      }
    }
  }
Comment: Compute the multipole coefficients from the charge vector q.
Comment: order is the order of the multipole expansion (typically 2).
  For each level j = L to 2 {
    For each level j cube i = 1 to 8^j {
      If cube i contains more than (order + 1)^2 panels {
        Compute the multipole coefficients for cube i using
        panel charges and/or coefficients of child cube multipole
        expansions.
      }
    }
  }
Comment: Compute the potential due to distant panels.
  For each finest-level cube i = 1 to 8^L {
    For each cube j in cube i's multipole list {
```

```
        If cube j contains more than (order + 1)^2 panels {
          For each panel k in cube i {
            Evaluate the multipole expansion for cube j at
            (x_k, y_k, z_k) and add to p_k.
          }
        }
        Else {
          For each panel k in cube i {
            For each panel l in cube j {
              Add P_kl q_l to p_k.
            }
          }
        }
      }
    }
```

It should be again noted that, as mentioned at the end of Section III, Algorithm 2 is a simplified version of the hierarchical multipole algorithm [14, 7] used in FASTCAP [1]. The complete algorithm also adaptively applies local expansions to improve the efficiency of the process of gathering together multipole expansions.

4.3. Comparison to Previous Work

The above approach to making the multipole algorithm adaptive is specialized to the boundary-element problem. A more general, but not as efficient, approach would be to extend to three-dimensions the two-dimensional adaptive algorithm described in [14]. In this earlier work, the multipole algorithm is made adaptive by breaking up the problem domain nonuniformly, in which case lowest level squares are of different sizes, where the size is chosen so that each lowest-level square has roughly the same number of panels.

To see why an adaptive algorithm based on a nonuniform partitioning of the problem domain can be inefficient, consider computing the potential at the center of the panel labeled **A** in Figure 4a. For this example, a two-dimensional square problem domain has been recursively quartered, the recursion being halted when a square had no more than one panel. To compute the potential at the center of panel **A** using a multipole algorithm based on this nonuniform partitioning requires: nine direct potential evaluations, for the nine panels in nearest-neighbor squares bordering the square containing **A**, and eleven multipole evaluations for the eleven nonempty squares not bordering **A**. Alternatively, if a uniform partitioning is used, as in Figure 4b, then it is easily seen that only *five* multipole evaluations are required.

Such an increase in computational cost can not occur with the adaptive algorithm given above, as the following theorem states:

Theorem 1 *The computational cost of the adaptive approach given in Algorithm 2 is never greater than that of the corresponding nonadaptive algorithm.*

The proof follows directly from the fact that the adaptive multipole algorithm, Algorithm 2, evaluates the potential due to panel charges in a cube directly, rather than with a

(a) (b)

Fig. 4. Partitionings used in Algorithm 2, (b), and by the adaptive algorithm of [14], (a).

multipole approximation, whenever the number of expansion coefficients would exceed the number of panels.

It should be noted that the overhead cost of maintaining a uniform domain partitioning has been ignored in this comparison. If the distribution of panels is very nonuniform, a matching nonuniform partitioning, like the approach used in [14], will naturally generate fewer lowest-level partitions, and hence reduce bookkeepping overhead. Careful data organization can make this overhead negligible for typical capacitance calculation problems. In the examples presented in Section VI, for which FASTCAP generates uniform domain partitionings with as many as $250,000$ lowest-level cubes, the bookkeepping overhead is never significant.

V. Preconditioning the Iterative Method

In general, the GMRES iterative method applied to solving (2) can be significantly accelerated by *preconditioning* if there is an easily computed good approximation to the inverse of P. We denote the approximation to P^{-1} by $\tilde{C}$, in which case preconditioning the GMRES algorithm is equivalent to using GMRES to solve

$$P\tilde{C}x = \overline{p}. \tag{20}$$

for the unknown vector x, from which the charge density is computed by $q = \tilde{C}x$. Clearly, if $\tilde{C}$ is precisely P^{-1}, then (20) is trivial to solve, but then $\tilde{C}$ will be very expensive to compute.

5.1. A Simple Example

A good approximation to P^{-1} that is easily computed, and fits with the hierarchical multipole algorithm described previously, can be derived by exploiting the fact that P^{-1} is

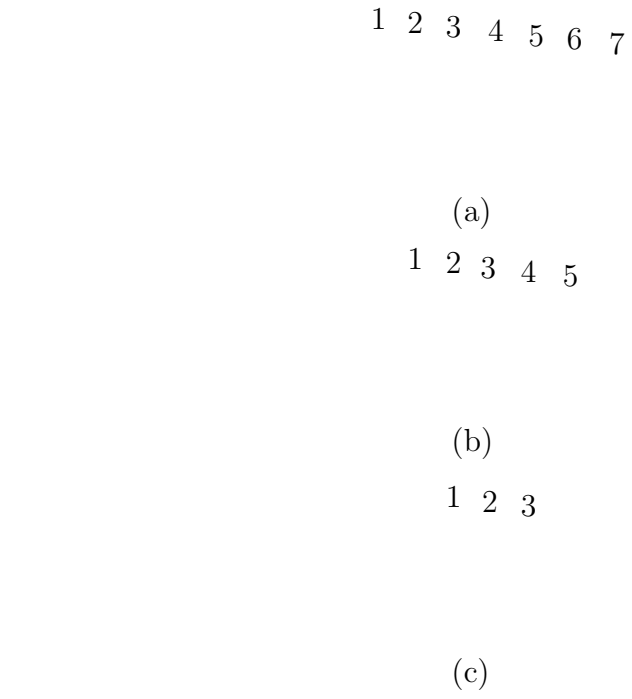

Fig. 5. Simple panel systems with potential coefficient matrices $P(7)$, (a), $P(5)$, (b), and $P(3)$, (c). The parallel, 1m×1m panels are spaced 0.5m appart.

approximately the *detailed* capacitance matrix, by which we mean the $n \times n$ capacitance matrix for the problem in which every panel or tile used to represent the conductor surfaces is treated as an independent conductor. To see why this point of view leads to a preconditioner, consider the 7×7 P matrix, denoted $P(7)$, for the seven panel example in Figure 5a. The fourth row of $P(7)$, which is associated with the center panel in Figure 5a, can be computed using the definition in (3) and is, in inverse-farads,

$$\begin{array}{ccccccc} P(7)_{4,1} & P(7)_{4,2} & P(7)_{4,3} & P(7)_{4,4} & P(7)_{4,5} & P(7)_{4,6} & P(7)_{4,7} \\ 0.5785 & 0.8346 & 1.4261 & 3.1686 & 1.4261 & 0.8346 & 0.5785 \end{array} \tag{21}$$

where all the values have been multiplied by 10^{-10}. The fourth row of $P(7)^{-1}$ is, in picofarads,

$$\begin{array}{ccccccc} P(7)^{-1}_{4,1} & P(7)^{-1}_{4,2} & P(7)^{-1}_{4,3} & P(7)^{-1}_{4,4} & P(7)^{-1}_{4,5} & P(7)^{-1}_{4,6} & P(7)^{-1}_{4,7} \\ -1.3080 & -1.5898 & -15.4544 & 46.7864 & -15.4544 & -1.5898 & -1.3080 \end{array} \tag{22}$$

From the definition in (3), the matrix elements $P_{4,j}$ must decay as $|j-4|$ grows, but notice that the terms in $P^{-1}_{4,j}$ decay *much faster* as $|j-4|$ increases. Viewing P^{-1} as an approximation to the detailed capacitance matrix makes clear that the very fast decay of terms in $P(7)^{-1}$ is just an example of classical electrostatic screening. The effect of screening can also be seen by examining the row of $P(5)^{-1}$ associated with the center panel in the five panel problem in Figure 5b and in the row of $P(3)^{-1}$ associated with the center panel in the three panel problem in Figure 5c, which are, in picofarads,

$$\begin{array}{ccccc} P(5)^{-1}_{3,1} & P(5)^{-1}_{3,2} & P(5)^{-1}_{3,3} & P(5)^{-1}_{3,4} & P(5)^{-1}_{3,5} \\ -2.1593 & -15.5547 & 46.6990 & -15.5547 & -2.1593 \end{array} \tag{23}$$

and

$$\begin{array}{ccc} P(3)^{-1}_{2,1} & P(3)^{-1}_{2,2} & P(3)^{-1}_{2,3} \\ -16.5499 & 46.4573 & -16.5499 \end{array} \tag{24}$$

respectively. Comparing (22), (23) and (24) leads to the observation that a good estimate for the fourth row of $P(7)^{-1}$ can be derived from the third row of $P(5)^{-1}$, which is a *smaller* problem, and that even the second row of $P(3)^{-1}$ provides a reasonable estimate. Specifically, the estimate based on the five-panel problem is

$$\tilde{C}_{4,j} = \begin{cases} P(5)^{-1}_{3,3+(j-4)}, & |j-4| < 3; \\ 0, & \text{otherwise}; \end{cases} \tag{25}$$

where $\tilde{C}$ denotes the estimate to $P(7)^{-1}$.

5.2. Preconditioning Algorithm

The above example suggests an approach to estimating P^{-1} for a general configuration of panels which fits with the hierarchical multipole algorithm in that the preconditioner $\tilde{C}$ can be constructed and applied in a cube-by-cube fashion. The preconditioner is formed by inverting a sequence of reduced P matrices, one associated with each finest-level cube, as in Algorithm 3 below.

Algorithm 3: Forming $\tilde{C}$.
For each finest-level cube $i = 1$ to 8^L {
Form P^i, the potential coefficient matrix for the
reduced problem considering only the panels contained
in cube i and cube i's neighbors.
Compute $\tilde{C}^i = (P^i)^{-1}$.
For each panel k in cube i or cube i's neighbors {
if panel k is not in cube i {
delete row k from $\tilde{C}^i$.
}
}
}

Note that $\tilde{C}^i$ is not a square matrix and that

$$\sum_{i=1}^{8^L} (\#\ \ rows\ in\ \ \tilde{C}^i) = n \tag{26}$$

where again n is the total number of panels. By comparing Algorithm 3 with Algorithm 2, it is clear that P^i uses only those elements of the full P matrix which are already required in Algorithm 2, and therefore the computational cost in computing the preconditioner is only in inverting small P^i matrices. Then computing the product $P\tilde{C}x^k$, which would be used in a GMRES algorithm applied to solving (20), is accomplished in two steps. First, the preconditioner is applied to form $q^k = \tilde{C}x^k$ using Algorithm 4 below. Then, Pq^k is computed using Algorithm 2 in the previous section.

Algorithm 4: Forming $q = \tilde{C}x$.

```
For each finest-level cube i = 1 to 8^L {
  For each panel j in finest-level cube i {
    For each panel k in cube i or its neighbors {
      Add C̃^i_jk x_k to q_j.
    }
  }
}
```

VI. Experimental Results

In this section, results from computational experiments are presented to demonstrate the efficiency and accuracy of the preconditioned, adaptive, multipole-accelerated (PAMA) 3-D capacitance extraction algorithm described above. In particular, the program FASTCAP, which can use both direct factorization and multipole-accelerated techniques, has been developed and incorporated into MIT's MEMCAD (Micro-Electrical-Mechanical Computer-Aided Design) system [9]. The structures described below were created with the solid modeling program in the MEMCAD system, PATRAN, or by computer program, and all capacitance calculations were performed using FASTCAP. The multipole-accelerated algorithms in FASTCAP use, by default, second-order multipole expansions and a GMRES convergence tolerance (see Algorithm 1) of 0.01.

Fig. 6. The sphere1 discretization of the unit sphere.

To demonstrate absolute accuracy, the FASTCAP program was used to compute the capacitance of a unit sphere, discretized as in Figure 6, and a unit cube, discretized as in Figure 7. In Table I, the capacitances computed using the PAMA algorithm are compared with the capacitances computed using direct factorization of P in (2) (Direct), and with

Fig. 7. The cube1 discretization of the unit cube.

Method	Problem	
	Sphere1 768 panels	Cube1 150 panels
Direct	110.6	73.26
PAMA	110.5	73.28
Other	111†	73.5,73.4

TABLE I Capacitance values (in pF) illustrating FASTCAP's accuracy. †By analytic calculation. ‡From [11] [15].

analytic results for the unit sphere and with reference results for the unit cube. As can be seen from the table, the results using the PAMA algorithm are easily within one percent of the analytic or reference results.

The PAMA algorithm is nearly as accurate as the direct factorization method even on more complex problems, such as the 2×2 woven bus structure in Figure 8. The capacitances computed using the two methods are compared in Table II, using coarse, medium, and fine discretizations of the woven bus structure, also shown in Figure 8. Note that the coupling capacitance C_{12} between conductors one and two, which is forty-times smaller than the self-capacitance C_{11}, is computed nearly as accurately with the PAMA algorithm as with direct factorization.

The computational cost of using the FASTCAP program is roughly proportional to the product of the number of conductors, m, and the number of panels n. This is experimentally verified using a parameterized version of the woven bus structure in Figure 8, that is, the

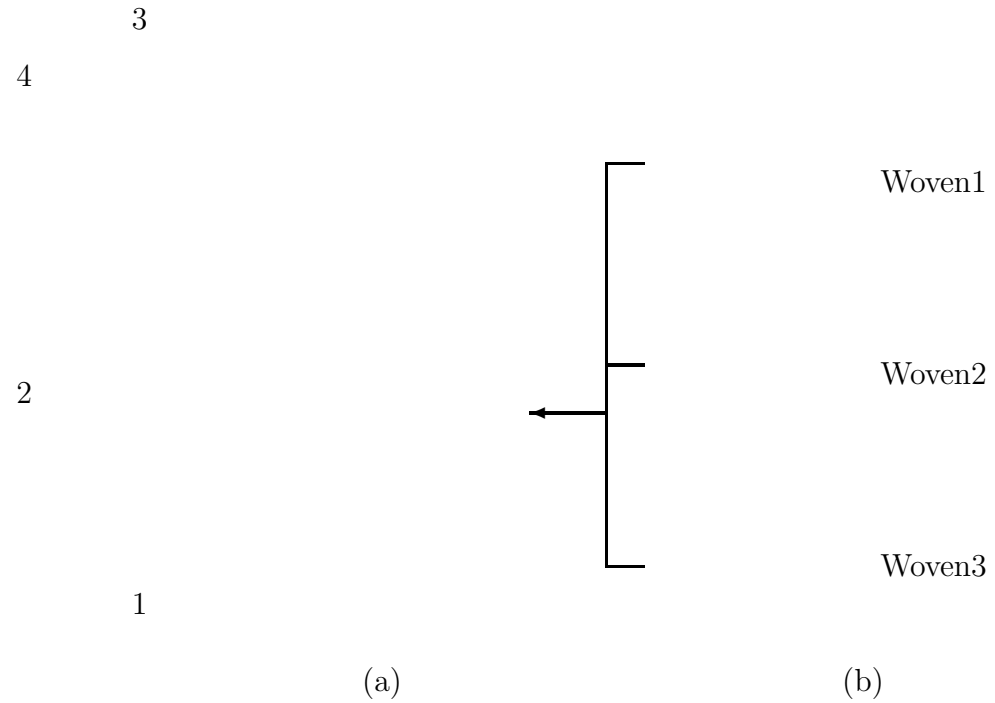

Fig. 8. The 2×2 woven bus problem: bars have 1m×1m cross sections. The three discretizations are obtained by replacing each square face in (a) with the corresponding set of panels in (b).

Method	Problem					
	Woven1 1584 Panels		Woven2 2816 Panels		Woven3 4400 Panels	
	C_{11}	C_{12}	C_{11}	C_{12}	C_{11}	C_{12}
Direct	251.6	−6.353	253.2	−6.446	253.7	−6.467
PAMA	251.8	−6.246	253.3	−6.334	253.9	−6.377

TABLE II Capacitance values (in pF) illustrating FASTCAP's accuracy for the complicated geometry of Figure 8.

Fig. 9. CPU time as a function of problem size times number of conductors, mn, for the PAMA algorithm applied to woven buses of various sizes. The dashed line is the least-squares best fit to the illustrated data points.

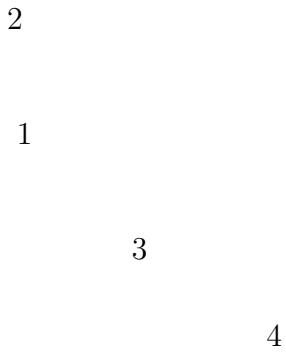

Fig. 10. Two signal lines passing through conducting planes; via centers are 2mm appart.

Fig. 11. A schematic illustration of the diaphragm problem. The two plates are 0.02μm appart at the center.

structure is extented to make a 3×3 bus, a 4×4 bus and a 5×5 bus, with surfaces discretized as depicted in the $Woven1$ example of Figure 8. In Figure 9, the CPU times for computing the capacitances of the woven bus structures are plotted as a function of mn, and as the graph clearly demonstrates the computation time does grow linearly.

To demonstrate the effectiveness of various aspects of the PAMA algorithm on a range of problems, in Table III the CPU times required to compute the capacitances of six different examples using four different methods are given. The examples Cube2 and Sphere2 are finer discretizations of the unit cube and sphere in Figures 6 and 7; the examples 2×2 Woven Bus and 5×5 Woven Bus are described above; the example Via, shown in Figure 10, models a pair of connections between integrated circuit pins and a chip-carrier; and the example Diaphragm, shown in Figure 11, is a model for a microsensor [16].

From Table III, it can be seen that using the adaptive multipole algorithm (AMA) typ-

ically reduces the computation time by a factor of two over using the multipole algorithm (MA) alone, and that using the preconditioner can reduce the computation time as much as a factor of three. Also, note that the PAMA algorithm is more than two orders of magnitude faster than direct methods for the larger problems.

Fig. 12. The GMRES residual norms for the linear system solution corresponding to the Diaphragm problem (Figure 11) with the top conductor at unit potential. As is evident here, the AMA method generally makes the iterate calculation more efficient, while the PAMA algorithm leads to fewer iterations.

The reduction in execution time afforded by the adaptive algorithm is due to increased efficiency in calculating each iterative loop iteration, rather than in a reduction the total number of iterations. The convergence plot in Figure 12 correspond to one of the linear system solutions associated with the Diaphragm problem and is representative of the general case. As is evident in the figure, the AMA algorithm generally computes nearly identical iterates to those calculated by the MA method but is faster, as reported in Table III. In contrast, the preconditioner leads to shorter computation time by reducing the total number of iterations rather than making each iterate calculation less costly. In fact one PAMA iterate requires more computation than an AMA iterate, but the difference is more than offset by the reduction in total number of iterations, as is certainly the case in Figure 12.

Method	Cube2 294 Panels	Sphere2 1200 Panels	2x2 Woven Bus 4400 Panels	Via 6185 Panels	Diaphragm 7488 Panels	5x5 Woven Bus 9630 Panels
Direct	0.11	3.2	185	(490)	(890)	(1920)
MA	0.06	0.3	6.0	11	8.7	42
AMA	0.05	0.2	3.3	4.7	5.9	23
PAMA	0.05	0.2	2.3	3.2	1.3	11

TABLE III CPU times in minutes on an IBM RS6000/540, times in parentheses are extrapolated.

VII. Conclusions and Acknowledgements

In this paper several new algorithms were presented that make multipole-accelerated three-dimensional capacitance calculation applicable and computationally efficient for almost any geometry of conductors in a homogeneous dielectric medium. In particular, a new adaptive multipole algorithm was described, along with a strategy for accelerating iterative algorithm convergence by exploiting electrostatic screening. Results from using FASTCAP, our program based on these techniques, to compute the capacitance of a wide range of examples were given, and they demonstrated that the new algorithms are nearly as accurate as the more standard direct factorization approach, and are more than two orders of magnitude faster for large examples. Current research in progress is in extending the above approach to solving problems with piecewise-constant dielectrics and ground planes.

The authors would like to thank Prof. Senturia for many valuable discussions on various approaches to preconditioning, and for his and Brian Johnson's help in linking FASTCAP with the M.I.T. MEMCAD system. The authors would also like to thank David Ling and Albert Ruehli of the I.B.M. T. J. Watson Research Center for their helpful suggestions about capacitance calculations. In addition, we would like to acknowledge the help of the members of the M.I.T. custom integrated circuits group. Finally, we are indebted to several anonymous reviewers for their careful evaluations of an earlier draft of this paper.

References

[1] K. Nabors and J. White, "Fastcap: A multipole accelerated 3-D capacitance extraction program," *IEEE Transactions on Computer-Aided Design of Integrated Circuits and Systems*, vol. 10, pp. 1447–1459, November 1991.

[2] R. F. Harrington, *Field Computation by Moment Methods*. New York: MacMillan, 1968.

[3] S. H. Crandall, *Engineering Analysis*. New York: McGraw-Hill, 1956.

[4] L. Collatz, *The Numerical Treatment of Differential Equations*. New York: Springer-Verlag, third ed., 1966.

[5] C. A. Brebbia, J. C. F. Telles, and L. C. Wrobel, *Boundary Element Techniques*. Berlin: Springer-Verlag, 1984.

[6] L. Greengard and V. Rokhlin, "A fast algorithm for particle simulations," *Journal of Computational Physics*, vol. 73, pp. 325–348, December 1987.

[7] L. Greengard, *The Rapid Evaluation of Potential Fields in Particle Systems*. Cambridge, Massachusetts: M.I.T. Press, 1988.

[8] V. Rokhlin, "Rapid solution of integral equations of classical potential theory," *Journal of Computational Physics*, vol. 60, pp. 187–207, September 15, 1985.

[9] F. Maseeh, R. M. Harris, and S. D. Senturia, "A CAD architecture for microelectromechanical systems," in *IEEE Micro Electro Mechanical Systems*, (Napa Valley, CA), pp. 44–49, 1990.

[10] S. M. Rao, T. K. Sarkar, and R. F. Harrington, "The electrostatic field of conducting bodies in multiple dielectric media," *IEEE Transactions on Microwave Theory and Techniques*, vol. MTT-32, pp. 1441–1448, November 1984.

[11] A. E. Ruehli and P. A. Brennan, "Efficient capacitance calculations for three-dimensional multiconductor systems," *IEEE Transactions on Microwave Theory and Techniques*, vol. 21, pp. 76–82, February 1973.

[12] Y. Saad and M. H. Schultz, "GMRES: A generalized minimal residual algorithm for solving nonsymmetric linear systems," *SIAM Journal on Scientific and Statistical Computing*, vol. 7, pp. 856–869, July 1986.

[13] J. D. Jackson, *Classical Electrodynamics*. New York: John Wiley & Sons, second ed., 1975.

[14] J. Carrier, L. Greengard, and V. Rokhlin, "A fast adaptive multipole algorithm for particle simulations," *SIAM Journal on Scientific and Statistical Computing*, vol. 9, pp. 669–686, July 1988.

[15] M. A. Jaswon and G. T. Symm, *Integral Equation Methods in Potential Theory and Elastostatics*. London: Academic Press, 1977.

[16] B. P. Johnson, S. Kim, S. D. Senturia, and J. White, "MEMCAD capacitance calculations for mechanically deformed square diaphragm and beam microstructures," in *Proceedings of Transducers 91*, June 1991.